Experimental Study of Turbulent Diffusion Flame Structure and Its Similarity*

Tamio IDA** and Kazutomo OHTAKE***

The interaction between reaction and turbulent mixing strongly affects the structures of a turbulent diffusion flame, the characteristics of which are greatly affected by the combination of working conditions such as burner exit configurations, burner size, fuel and oxidant. This study discusses in detail the turbulent diffusion flame structure and its similarity using a laboratory-scale turbulent diffusion flame measured by laser Rayleigh scattering. It also discusses the factors affecting the similarity in flame structure and the turbulent diffusion flame length determined using its turbulent power spectral density. The $-5/3$ power law holds in the fuel jet and combustion regions but in the air entrainment regions, the $-5/3$ and -1 power laws coexist, and which shows that both turbulent and molecular thermal diffusions become important. The constancy of the turbulent diffusion flame length at a high Reynolds number is discussed with respects to the characteristics of flame structure.

Key Words: Turbulent Diffusion Flame Structure, Laser Rayleigh Scattering, Power Spectral Density, Flame Length, Similarity of Turbulent Flame Structure

1. Introduction

A detailed study of turbulent diffusion flame structures is very important in order to understand the interactions between chemical reaction and turbulent mixing. In particular, a study on the similarity between turbulence structures in flames is essential not only to elucidate the macroscopic transportation mechanisms of heat and mass in turbulent combustion but also to correlate the independent experimental results reported by different researchers. One of the most important points in studying the similarity law existing in turbulent diffusion flame structures is to determine the common occurring in the flames.

Turbulent diffusion flames have been studies mostly by space and time mean measuring methods in order to derive statistical and semi-quantitative descriptions. Typical adopted instrumentations have been schlieren photography and a fine hot wire[1),(2)]. As one of the typical characteristics of turbulent diffusion flames, Beér and Chigier[3] proposed a formula to calculate flame length using the density of combustion gas at the adiabatic flame temperature, but this formula could not describe the flame structure. On the other hand, Becker and Liang[1] showed that the turbulent diffusion flame length did not depend on the Reynolds number (Re number), as Hottel and Hawthorne[2] suggested, but was closely related to the Froude number (Fr number). Pearson et al.[4] introduced an acoustic excitation method to produce a turbulent diffusion flame and discussed the change of flame structure based on schlieren photography and pointed out the necessity to study instantaneous flame structures. Flame structures are affected by many non-dimensional numbers governing the phenomena such as Re and Fr numbers, and Prandtl number (Pr number). It is important to discuss turbulent diffusion flame structures in order to develop a new model.

Dibble and Hollenbach (1981)[5] and Schoenung

* Received 1st March, 1996. Japanese original: Trans. Jpn. Soc. Mech. Eng., Vol. 61, No. 582, B (1995), pp. 744-751 (Received 22nd April, 1994)

** Kumano Technical College, Department of Mechanical Engineering, 2800 Arima-cho, Kumano, Mie 519-43, Japan

*** Toyohashi University of Technology, Department of Ecological Engineering, 1-1 Tempaku-cho, Toyohashi, Aichi 441, Japan

Table 1 The characteristics of flame structures in four regions

Region	Characteristics of flame structures
I	This region exists in the central region of the flame where homogeneous temperature fluctuation is produced by heat transportation based on the turbulent diffusion of the heat and combustion products in the combustion regions.
II	This region exists just outside Region I. The maximum time mean temperature appears, and the time scale of temperature fluctuation steeply increases. These show that the entrained air penetrates into this region and combustion takes place at the interface between fuel and air.
III	This region shows the characteristics that the time mean temperature steeply decreases while the time scale of temperature fluctuation is kept almost constant. This region could be defined as the region where the outside air flow is entrained into the flame region by the large scale eddies produced by the buoyancy of hot combustion gas.
IV	The air flow region surrounding the flame.

and Hanson(1982)[6] studied non-premixed turbulent flames using a laser Rayleigh scattering method and discussed the difference in flame structure between turbulent non-premixed and premixed flames. They obtained the power spectral density (PSD) and other statistical values. Five kHz was the higher limit of frequency response of their diagnostics and it still remains a blind part of the phenomena occurring in the higher frequency region.

Lockwood and Odidi(1984)[7] presented the time scale of the ion concentration fluctuation in turbulent flames measured using an ionization probe. The ionization probe technique could give information on reaction fluctuations, but the affect of inserting solid probes into rather small flames might be questionable.

In this study, time-resolved signals and the PSD of temperature fluctuations up to 10 kHz were obtained by means of laser Rayleigh spectroscopy (LRS) which had no direct effect on the flame during the measurement. The effects of the burner diameter and *Re* number on turbulent diffusion flames structures are discussed based on similarities of flame structures. The flames could be classified into four regions based on the characteristics of LRS signals and their statistical values. The reason why the length of the turbulent flame is kept constant for different burner exit velocities is discussed with respect to the phenomena occurring in these regions. The characteristics of the flame structures in the four regions which were clarified in the previous study are summarized in Table 1.

2. Experimental Apparatus and Procedures

Figure 1 shows the layout of the experimental apparatus. The flame temperature was measured by LRS using a laser light with a wave length of 488 nm injected by an Ar ion laser as a light source. This

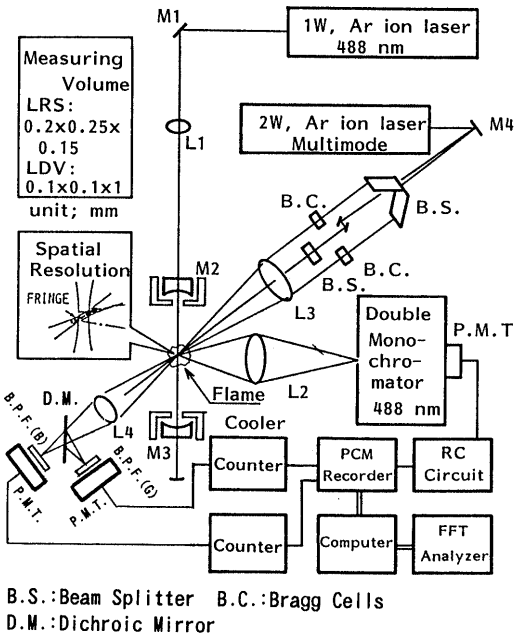

Fig. 1 Layout of experimental apparatus

system can detect the temperature fluctuations up to 10 kHz, and is considered to be a useful diagnostic for measuring turbulent diffusion flame structures. In particular, a pair of spherical multi-reflection mirrors reflected the laser light about ten times in order to intensity the incident light strength at a focused point.

Coaxial turbulent diffusion flames at moderate Reynolds number, which maintain typical diffusion flame structures, were formed on laboratory-scale burner. A mixed gaseous fuel of 62.2% H_2+37.8% CH_4 was fed to the burner, the inner diameters of which were 2 and 4 mm, and surrounded by a coaxial air duct of 64 mm I. D. The Rayleigh scattering cross-section of this fuel does not change more than 5% from those of air, fuel and combustion gas before,

Table 2 The experimental conditions

Mixed fuel	62.2%H_2+37.8%CH_4	
Burner size (mm)	Reynolds number (-)	Velocity (m/s)
2	2, 000	36. 9
	2, 500	46. 2
	3, 000	55. 4
	5, 000	92. 3
4	5, 000	46. 2
	7, 000	64. 7
	10, 000	92. 3

Table 3 Specification of the 2C4BLDV optical system

Wave length (nm)	488	514.5
Cross angle(mdeg.)	45.9±0.35	49.4±0.35
Beam diameter (mm)	0.1(e^{-2})	0.2(e^{-2})
Spatial resolution (mm^3)	0.1x0.1x2 0.02	0.2x0.2x4 0.16
Fringe interval (μm)	5.32±0.04	5.21±0.04
Fringe number	20±1	38±1

during and after combustion. Table 2 shows experimental conditions which were prepared to divide the roles of the Re number and exit fuel velocity.

A two color and four beam forward scattering 2 W ion laser-sourced LDV system (2C4BLDV) at 488 and 514.5 nm in wavelength was used simultaneously with the LRS system to measure axial and radial velocities, respectively. Talcum powder with a nominal diameter of 2 μm was used as the seeding particle for LDV. The specification for the 2C4BLDV optical system is summarized in Table 3. The light intensity scattered from the measuring volume was converted into electric signals by a photomultiplier and recorded by a PCM recorder after treatment by a counter-type LDV signal processor. The successive 200 000 data points (corresponding to 4 seconds in real time) from the recorded signal and the data sampling frequency, at 50 kHz, were used to obtain statistical values of turbulent flame structures using an FFT analyzer and computers.

3. Results and Discussion

3.1 Basic Structure of Turbulent Diffusion Flame

The obtained distributions of the root mean square of temperature fluctuation, T_{rms}, over almost the whole flame area in a standard flame (D=2 mm, Re=5 000) are shown in Fig. 2. The original of the direction is taken as the central axis of the burner and that of x as the burner tip, respectively. The corresponding time mean averaged temperature distribution was shown elsewhere[8]. It can be observed that T_{rms} has peaks across the maximum T_{mean}. The positions of these two peaks of T_{rms} correspond well to the positions of the maximum gradient of T_{mean}, which shows the validity of the gradient model of the statistical time mean value of temperature.

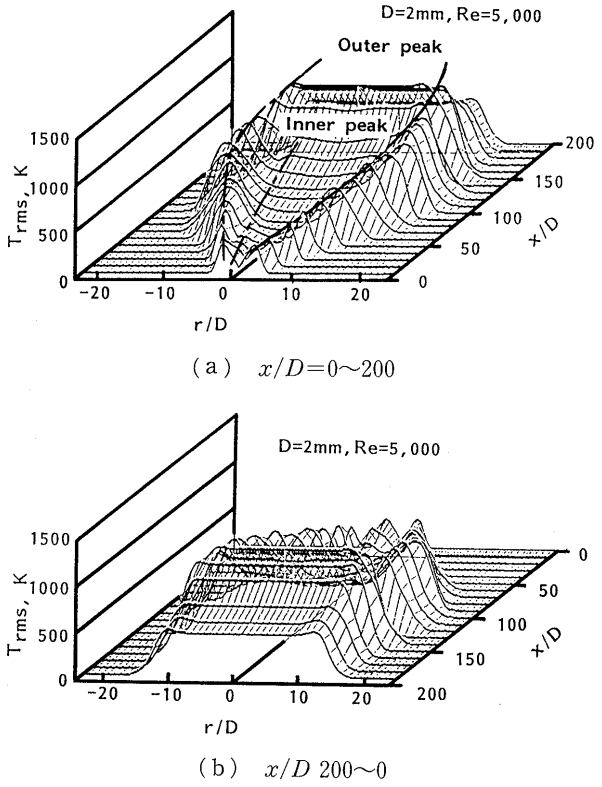

Fig. 2 Distributions of root mean square of temperature fluctuation for the whole flame area in a standard flame (D=2 mm, Re=5 000)

The peak value of T_{rms} outside the maximum time mean temperature is higher than that inside. This indicates that the amplitude of temperature fluctuation outside the maximum T_{mean} is larger than that inside because the entrainment of air flowing outside the flame produces a large temperature difference between the burning zone formed along the periphery of the fuel rolls, branches and/or islands. In contrast, inside the maximum T_{mean} the velocity difference between the fuel and the burning zone is not so large when x/D attains a certain value. For example 10, the eddy size could not be large and the transported eddy of the burned gas into the fuel flow the burning zone becomes small. Furthermore, the temperature difference between the eddy and the fuel flow is not so large because the fuel flow increases its temperature very quickly due to the turbulent heat transfer from the upstream burning region. These phenomena cause the value of T_{rms} inside the maximum T_{mean} to be lower than that outside. The air

entrainment from outside the flame becomes stronger with increasing x and the spatial width of the region where T_{rms} appears also becomes wider because the entrained air should penetrate further into the combustion region and break its scale to assist the burning of unburned fuel. In the central region T_{rms} shows a flat distribution and omit its value gradually increases along the distance from the burner tip. These phenomena produce a peak value of T_{rms} at the outside which increases its value with distance from the burner tip until near the flame tip where the fed fuel has been consumed and both peaks of T_{rms} become connected. In contrast, the inside peak of T_{rms} decays quickly as the temperature increases.

This is caused by the consumption of fuel flow energy which accelerates nitrogen in air (79% in volume) at a slow velocity. The trend whereby the maximum value of T_{mean} is almost constant all over the flame indicates the presence of an intricate complex turbulent structure caused by successive turbulent diffusion flame processes such as the entrainment of surrounding air into fuel flow, the formation of a combustion region at the mixing periphery between fuel and air, and mixing with combustion gas. Furthermore, downstream of the top end of region I where most of the fuel has been consumed, the mechanism of entrainment of outside air changes significantly from that observed upstream. The turbulent scale increases so much because a combustion reaction does not exist. In this region the entrainment of large scale eddies of the surrounding air into combustion gas occurs. This entrainment influences the structures of the flame tip regions because the entrained air passes through region II where the combustion takes place between the unburned fuel and air with smaller eddies[9]. T_{rms} becomes larger and its distribution flatter when T_{mean} distributes more uniformly. This tendency becomes weaker when the distribution of T_{rms} becomes uniform. This phenomena suggests that this is the region where the Fr number becomes more important as the buoyancy force dominates with the increase of gas temperature from the region where the Re number mainly governs the phenomena just after the burner exit. From these results, the variation of T_{rms} can be considered as an important parameter for the evaluation of the thermo-fluid dynamic mixing process accompanied by chemical reaction. These discussion are quite useful for extending the understanding of local flame structures based on the results obtained in the previous paper[8] to comprehensive understanding of whole structures of turbulent diffusion flames.

Next, the gradient of PSD as a function of its frequency band is discussed in order to examine the

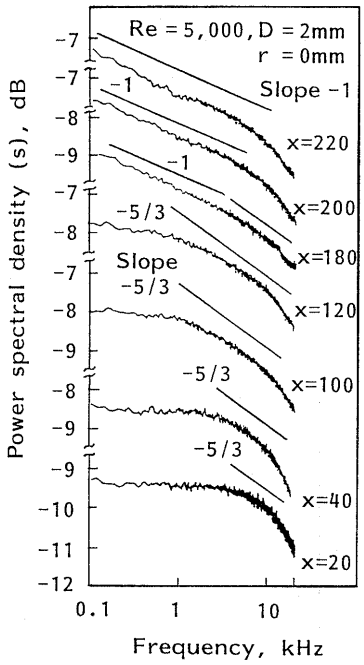

Fig. 3 PSD variations at various positions along the center axis of the flame (r/D=0, Re=5 000, D= 2 mm)

turbulent thermal diffusion and its variation as a function of frequency of temperature fluctuations. Figure 3 shows PSD variations at various positions along the center axis of the flame of Re=5 000 and D =2 mm. This figure clearly shows that the −5/3 power law, showing the turbulent thermal diffusion, appears at a higher frequency region until x/D=120. Downstream of this point, however, corresponding to the air entrainment regions, the −1 power law, which shows molecular thermal diffusion, starts to appear in a lower frequency region. As the height increases, the −1 power law begins to cover a wider frequency and shifts to a lower frequency region with increasing distance from the burner tip. This means that the turbulent heat transfer mechanism changes to a laminar heat transfer dominant mechanism as the steep velocity gradient in the main flow decreases.

In order to discuss the effect of thermal diffusion on the flame structure the PSD of temperature fluctuations at various radial positions at x/D=25 of the flame of Re=5 000 formed on the burner of D=4 mm are shown in Fig. 4. The results at x/D=25 for D= 2 mm are shown in Ref.(8). In regions I and II, the −5/3 power law, corresponding to the turbulent thermal transportation, covers the whole domain of the measured frequency region. In regions III and IV, the −5/3 and −1 power laws coexist and the frequency region covered by the latter law expands to a lower frequency region. The −1 power law appearing in the turbulent mixing zones in region III corresponds

to the molecular mixing phenomena occurring between the fuel in the central fuel flow and the air entrained from the surrounding air flow region IV. This differs in principle from the -1 power law which appears near the flame tip in region I. If the turbulence moves at 1 m/s, 5 kHz fluctuation indicates the existence of an eddy of 200 μm in size. The change of the turbulent diffusion flame structure by the burner Re number can be discussed from the results shown in Fig. 5. Although the distributes of PSD at three different Re numbers differ slightly at the central axis, they almost the same shape. The same results can be seen at a different distance from the burner tip. These results could explain the phenomenon in which the flame length of the turbulent diffusion flame is almost constant at different Re numbers. This phenomenon also expresses the fact that temperature fluctuations are not controlled by the fluid dynamic initial conditions given at the burner exit and the local mean velocity.

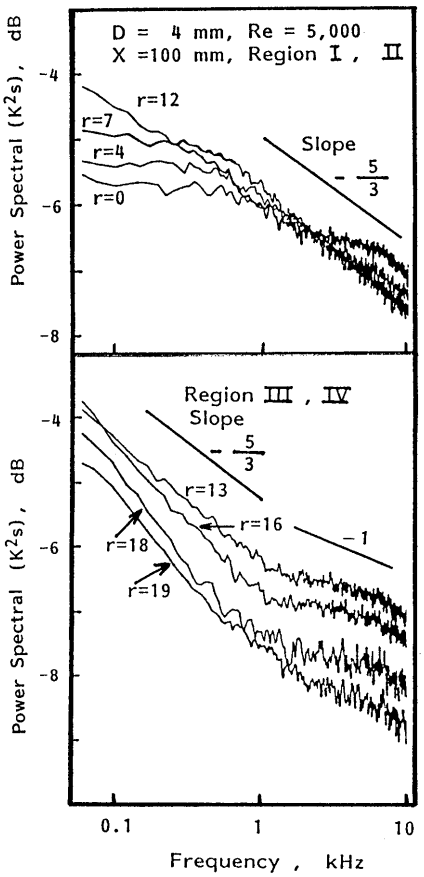

Fig. 4 PSD of temperature fluctuations at various radial positions (x/D=25, Re=5 000, D=4 mm)

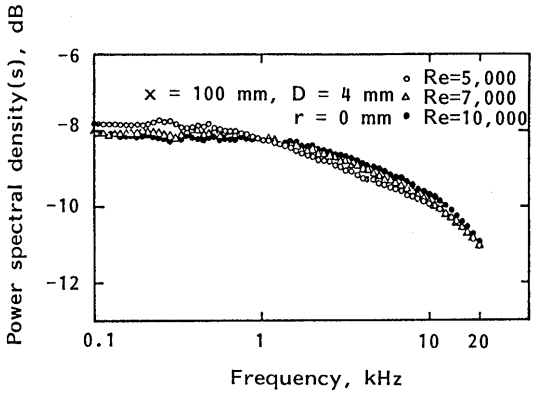

Fig. 5 PSD of temperature fluctuations at various Re numbers (r/D=0, x/D=25, Re=5 000, D=4mm)

The flame structures suggested by these results combined with the experimental results by Pearson et al.[4] indicate that the turbulent intensity of temperature fluctuation is influenced by the turbulent Re number at the burner exit (especially the velocity fluctuation in the main flow direction), but not by the local Re number ($\bar{U}D/\nu$), D: burner inner diameter, ν: kinematic viscosity at local temperature.

On the other hand, in order to discuss the turbulence in the velocity field, the radial distributions of time mean axial velocity component at Re=5 000, D =4 mm and x/D=10～25 are shown in Fig. 6. The radial distributions of the corresponding Reynolds stress are shown in Fig. 7. The radial distribution of turbulent heat flux in the radial direction, $\overline{v'T'}$, was obtained experimentally by simultaneous measurements of velocity and temperature using LDV and laser Rayleigh scattering methods, respectively[10]. From these results, the turbulent radial heat flux showed proportionalities to the spatial radial gradient of the time mean temperature $\partial\bar{T}/\partial r$ at almost all areas except the flame region (region II). This means that the simple turbulent model cannot be applied at the burning region especially near the point of the maximum time mean temperature. This fact indicates the necessity to clarify the thermo-fluid dynamic transportation mechanism in velocity and temperature fields with combustion reaction.

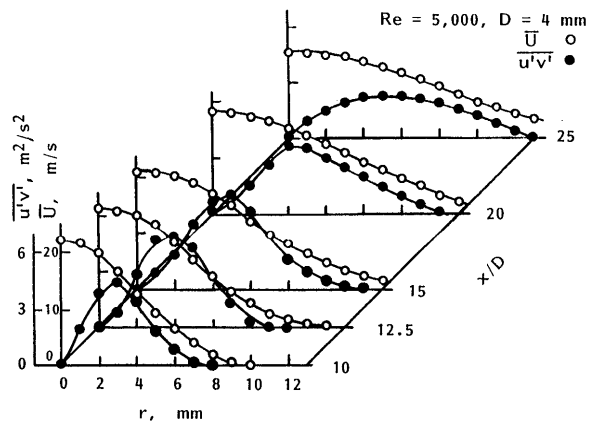

Fig. 6 Distribution of turbulent Reynolds stress

As shown in Fig. 6, the turbulent Reynolds stress is proportional to the radial gradient of time mean axial velocity in all regions. The turbulent kinematic viscosity obtained by dividing the Reynolds stress by the spatial radial of time mean axial velocity is shown in Fig. 7. The kinematic viscosity changes gradually in the axial and the radial directions, and increases its value near the central axis at the downstream region.

3.2 Variation of turbulent diffusion flame structure by burner exit Reynolds number

This section discusses the transition mechanisms from laminar to turbulent diffusion flames in a frequency plane by changing the burner Re number. In particular, by changing the burner Re number to maintain a constant burner exit diameter the influence of thermo-fluid dynamic heat transportation to the turbulent diffusion flame structure through the inertia term is described by variation of the PSD of temperature fluctuations.

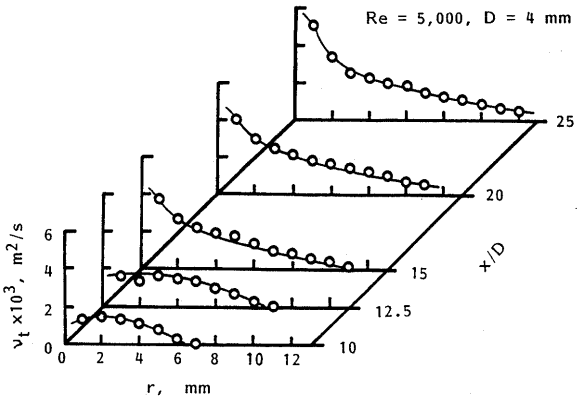

Fig. 7 Distribution of turbulent kinematic viscosity obtained by dividing Reynolds stress

Figure 8 shows time-dependent temperature signals at the central position (Region I) at $x/D=25$ of the burner of $D=2$ mm. At $Re=2\,000$, the fuel at room temperature flows at the measuring point under a laminar condition which has not yet been heated by hot combustion gas. At $Re=2\,500$, intermittency between laminar and turbulent temperature signals starts to appear. This means that the measuring point becomes a transition point and high temperature combustion gas frequently penetrates into the central region. When the Re number becomes higher than 3 000 the flame becomes turbulent and turbulent heat transportation from the burning region produces typical turbulent signals.

3.3 Time averaged temperature becomes higher and its temperature fluctuation smoother

Figure 9 shows variations of PSD as a function of frequency at various Reynolds numbers and x/D values. At $Re=2\,000$, the laminar flow characteristics are maintained until $x/D=25$ and -1 power law of molecular thermal diffusion covers all frequency ranges. At the downstream region of $x/D=50$, the

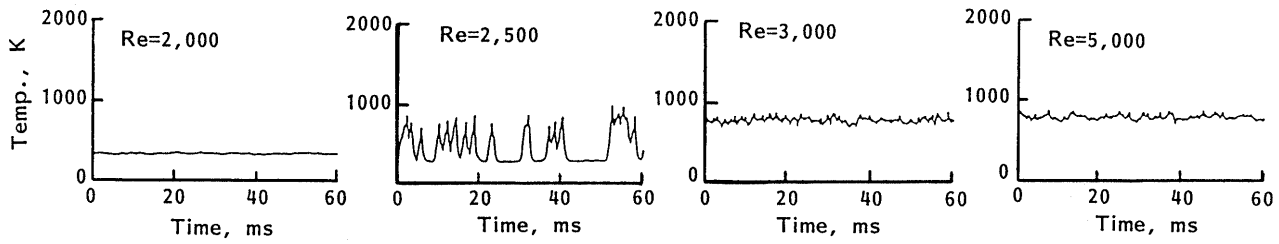

Fig. 8 Time-dependent temperature signals at various Reynolds numbers ($r/D=0$, $x/D=25$, $D=2$ mm)

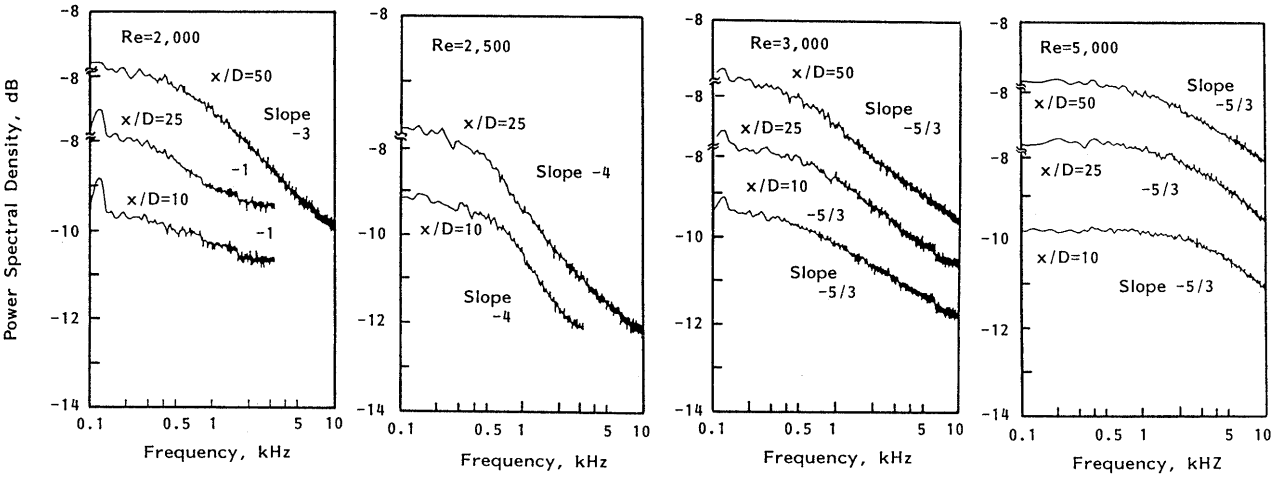

Fig. 9 The variations of PSD at various Reynolds numbers and x/D values

flow becomes turbulent and the -3 power law appears at a higher frequency region. When a turbulent Prandtl number is smaller than unity, the gradient of PSD shows a power law between -3 and -4 at a transition condition. At $Re=2\,000$ a transition from laminar to turbulent occurs near the measured point.

Furthermore, at the position of $x/D=50$, in the case of $Re=3\,000$ and $5\,000$, the $-5/3$ power law covers a considerably wide frequency range and this shows that the flow becomes completely turbulent. However, it may be difficult to use turbulent theory to provide a physical meaning or explanation of the structures of the present turbulent diffusion flames.

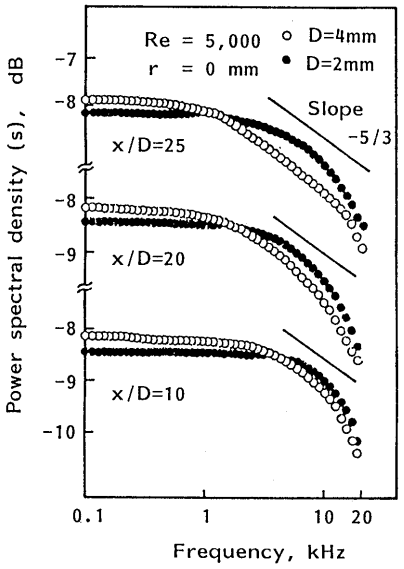

(a) Comparisons at the same x/D

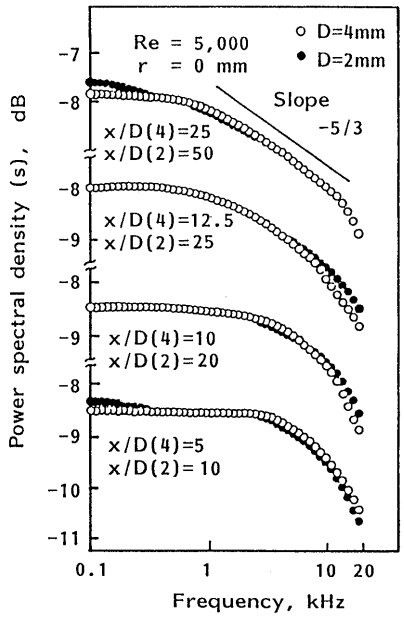

(b) Comparisons at the same x

Fig. 10 Similarity of turbulent structures as a function of burner diameter

3.4 Similarity of turbulent structures as a function of burner diameter and its Reynolds number

This section discusses the similarity of turbulent structures of studying flames as a function of burner diameter and its Re number. Traditionally, flame characteristics have been arranged as a function of x/D since the flame length is proportional to the burner diameter. In the previous report Ref.(9) it was shown that time mean values such as $\overline{T}$ and $\overline{U}$ could be arranged by this law. The characteristics of PSD for flames with different burner diameters are shown in Fig. 10. Comparisons are made at the same x/D in Fig. 10(a) and at the same x in Fig. 10(b). As shown in Fig. 10(a), PSDs at the same x/D do not fit with each other, but they do fit at the same distance from the burner tip as shown in Fig. 10(b). This certifies that the similarity factor is not the burner diameter even in a region where the flow field is governed by the turbulent law (the $-5/3$ power law). This fact elucidates that there is a region where the burner diameter could not be a similarity factor even though the flow field is governed by a burner Re number.

Finally, in order to compare turbulent structures, PSDs at $Re=5\,000$, $D=4$ mm and $x/D=25$ are shown in Fig. 11. The velocity fluctuations in the flow direction are cited here. It is observed in Fig. 11 that PSDs for temperature and velocity show the same tendencies in the region where the $-5/3$ power law is dominant. However, this agreement begins to break in the frequency region where the -1 power law

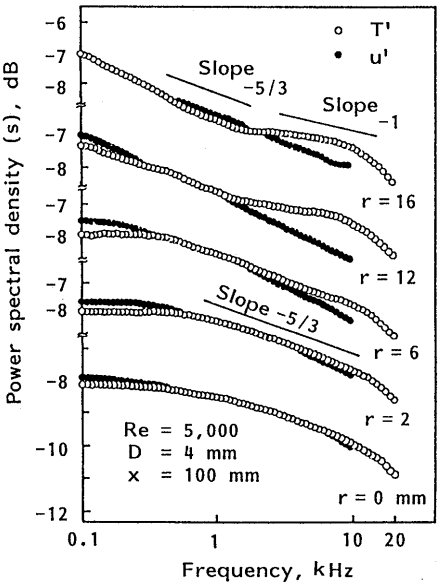

Fig. 11 Comparison of turbulent structures by PSDs for temperature and velocity ($D=4$ mm, $x/D=25$, $Re=5\,000$)

stands. The frequency at which the -1 power law starts shifts to a lower frequency when the radial distance increases. This suggests that in region III the frequency where the molecular heat conduction starts to be dominant differs from the frequency where molecular viscosity performs the main role. However, some unsolved problems may exist in the LDV measurement, especially in the velocity slip between the seeded particles and gas velocity, and further study is necessary to reach final conclusions.

4. Conclusions

The following conclusions regarding the characteristics of structures and the similarities of turbulent diffusion flames were derived by applying LRS and LDV systems for the temperature and velocity measurements, respectively.

(1) It was shown quantitatively from the PSD signals of temperature fluctuations that the shift from the inertia force dominated region (Reynolds number guides the phenomena) to the buoyancy force control region (Fr number is dominant) occurs near the burner exit.

(2) From the radial change of PSD characteristics, it was understood that the $-5/3$ power law (turbulent heat transportation based on fluid dynamic mixing) occupies most of the measured frequency range in Region I and II, while the $-5/3$ and -1 power laws (molecular thermal diffusion) coexist in Regions III and IV.

(3) The constancy of flame length independent of the burner Re number was explained from the similar features of PSDs.

(4) The shift of mixing mechanisms from laminar to turbulent was quantitatively shown by the PSD characteristics of various Re number.

Acknowledgment

This work was partly supported by a Grant-in-Aid for Scientific Research(B)(01627002) from The Ministry of Education, Science and Culture of Japan, which is greatly appreciated.

References

(1) Becker, H.A. and Liang, D., Combustion Flame, Vol. 32(1978), p. 25.
(2) Hottel, H.C. and Hawthorne, W.R., Proc. 3rd Symp. (Int.) Combust., (1949), p. 254.
(3) Beér, J.M. and Chigier, N.A., Combust. Aerodyn. (1974), p. 40, Robert E. Krieger
(4) Pearson, I.G., et al., Proc. Joint Int. Conf. Australia/NewZealand and Japanese Sections, The Combustion Institute, Sydney,(1987), p. 63.
(5) Dibble, R.W. and Hollenbach, R.E., 18th Symp. (Int.) Combust.,(1981), p. 1489.
(6) Schoenung, S.M. and Hanson R.K., 19th Symp. (Int.) Combust.,(1982), p. 449.
(7) Lockwood F.C. and Odidi A.O.O., 21th Symp. (Int.) Combust.,(1984), p. 561.
(8) Ida, T., Ohtake, K., Trans. Jpn. Soc. Mech. Eng., (in Japanese), Vol. 58, No. 550,B(1992), p. 1918.
(9) Ida, T., Ohtake, K., Trans. Jpn. Soc. Mech. Eng., (in Japanese), Vol. 56, No. 531, B(1990), p. 3514.
(10) Ida, T., Ohtake, K., Trans. Jpn. Soc. Mech. Eng., (in Japanese), Vol. 52, No. 482, B(1986), p. 3571.